2008 IEEE International Conference on
Robotics and Automation
Pasadena, CA, USA, May 19-23, 2008

Collision Avoidance Techniques for Tele-Operated and Autonomous Manipulators in Overlapping Workspaces

Andrew Spencer, Mitch Pryor, Chetan Kapoor and Delbert Tesar

***Abstract*—This paper describes the integration of several techniques for cooperative control of both tele-operated and autonomous redundant manipulators with overlapping workspaces. Motivating this research is a tele-operated surgical manipulator(s) supported by autonomous robot(s) that insert/remove items from the surgical workspace. The dynamic and unpredictable location of obstacles in a small workspace requires a complete strategy to avoid collisions when completing critical tasks and minimizes the need for user (i.e. the surgeon) intervention to make path planning decisions or resolve impasse situations. Three techniques are integrated into the decision-making for the manipulators: an intelligent and intuitive EEF velocity scaling, coordinated null-space optimization across affected manipulators, and collision detection. Central to all three techniques is an *estimated time-to-collision* formulation that combines distances between objects with their higher order properties, thus only objects currently moving towards each other are included in the collision avoidance techniques. The use of multiple techniques derived from the terms of a single metric results in a computationally efficient strategy for tele-operated and autonomous manipulators sharing the same workspace.**

I. Introduction

SURGEONS and scrub nurses complete varied and complex interactions that occur in rapid succession and in close proximity to the surgical site. The generally higher priority of tasks completed by the surgeon is understood, and yet the surgeon will inevitably shift his elbow, move to right, or even modify the orientation of his hands (task permitting) if the scrub nurse needs additional space to complete his prescribed task. The scrub nurse must be able to retrieve items from various locations around the surgical site and then present them into the surgeon's field of view from a direction that does not impede his vision and allows him to easily interact with the new items. In other words, the doctor and nurse must perform a continuous negotiation of how to share the limited workspace to complete a set of critical, unstructured tasks without collision or impasse.

There is a large body of body of work in robotics focusing on a manipulator's ability to complete tasks in cluttered, dynamically changing environments while avoiding collisions. Research topics in this area can be generally categorized as exploiting the null-space motion of redundant systems [1][2][3], etc., collision detection [4][5][6], off-line path planning [7][8], real-time path alteration [9][10], computational efficiency [11][12], self-collision [13][14], mobility [9], and human machine interaction [15][16]. Additionally, for tele-operated systems, researchers have evaluated *virtual fixtures* to assist the operator in avoiding collisions and/or target acquisition for the end-effector (EEF) [17][18].

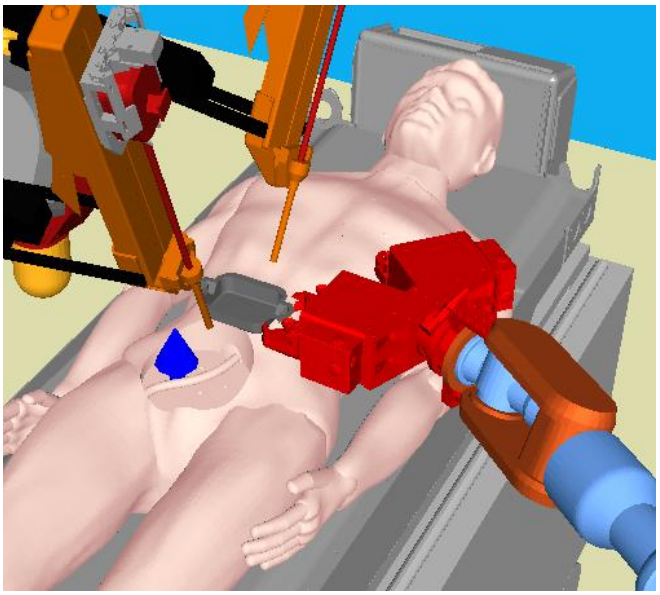

Fig. 1. An example of a surgical and nurse (support) manipulator in the compact surgical workspace.

Yet the application targeted in this research – tele-operated and autonomous manipulators sharing a small workspace – creates a unique subset of requirements that must be completely addressed by the collision avoidance strategy:

- Autonomous support manipulators must avoid not only all collisions, but also erratic motions that may lead the operator to suspect an imminent collision and delay a critical task.
- Autonomous support manipulators need to behave in an intuitive manner slowing down as they approach the surgical arms and moving away quickly when a task is done in order to free the workspace from obstacles and quickly prepare for their next task.
- In an enclosed workspace, the autonomous support

Manuscript received September 14, 2007. This work was supported in part by the U.S. Department of Energy under Grant DE-FG52-06NA25591 and DARPA/US-Army TATRC Grant W81XWH-05-2-0012.

Authors are with the Robotics Research Group at the University of Texas at Austin, TX 78758 USA (corresponding author's phone: 512-471-3039; fax: 512-471-3987; e-mail: mpryor@mail.utexas.edu).

manipulators will need to perform tasks to either side of the surgical workspace and approach the workspace with items from different entry locations as directed by the operator.

- The manipulators must be able to exchange tools or items in either direction in the compact workspace.

Some researchers have addressed aspects of these requirements in their research. Khatib [19] effectively applied a framework of conceptual elastic strips to an autonomous multi-robot workcell which added a reactive component to each robot in the workcell. He additionally showed how manipulator velocities could be tuned as a conflict resolution strategy. Although the proposed methods are effective for fully autonomous workcells, it may lead to unexpected motions and other unpredictable behaviors due to the high priority, tele-operated presence in the compact workspace (in contrast to the examined workcell in [19] where workspaces temporarily overlapped). Dubey [20] demonstrated sensor and model based velocity mapping to dynamically optimize the command ratio between a master and slave arm to perform a tele-operated docking task involving a single manipulator. Additionally, [21] developed a velocity-bounded *collidability metric* implemented in a dynamic control law potentially useful in compact workspaces since it "reduce[s] the magnitude of the obstacle avoidance action considerably, especially when manipulator links move away from obstacles."

II. Kinematic Framework

Thomas and Tesar [22] developed the Kinematic Influence Coefficients (KICs) representation for mapping system input to output parameters. KICs are useful for succinctly modeling multi-robot systems. The first order KICs (*G* functions) map the first derivative of joint angles with respect to time to the EEF velocity through the relationship

$$\dot{\overline{P}} = \left[G_{\overline{P}} \right] \dot{\overline{\theta}} = \begin{bmatrix} \left[G_{p(\overline{P})} \right] \\ \left[G_{jk(\overline{P})} \right] \end{bmatrix} \dot{\overline{\theta}} \tag{1}$$

where $\overline{\theta}$ is the joint position of the system, $\overline{P}$ is the output parameter and $\left[G_{\overline{P}} \right]$ is commonly known as the *Jacobian* and the matrices $\left[G_{p(\overline{P})} \right]$ and $\left[G_{jk(\overline{P})} \right]$ are the translational and rotational specific elements respectively. The second order KICs are referred to as *H* functions, which map the first and second derivatives with respect to time of the joint positions to the second derivative of the output parameter through the relationship

$$\ddot{\overline{P}} = \left[G_{\overline{P}} \right] \ddot{\overline{\theta}} + \dot{\overline{\theta}}^T \left[H_{\overline{P}} \right] \dot{\overline{\theta}} . \tag{2}$$

KICs are only a function of $\overline{\theta}$, meaning that they are determined only by the instantaneous geometry of the system and are equivalent for any time derivatives of $\overline{\theta}$.

Harden and Tesar [3] describe a modeling system for manipulators using cylisphere primitives – cylinders with spherical ends created by sweeping a radius around a line segment. Distance calculations between these primitives are compact and efficient requiring only the computation of a distance between two line segments. Using this primitive, the first order time derivative of the distance between two cylisphere primitives *i* and *j* (referred to as the closing velocity) between links on two moving manipulators can be described as

$$\dot{d}_{(i,j)} = \left[G_{di}^{(i,j)} \right] \dot{\overline{\theta}} + \left[G_{dj}^{(i,j)} \right] \dot{\overline{\phi}} \tag{3}$$

where $d_{(i,j)}$ is the distance between the primitives, $\left[G_{di}^{(i,j)} \right]$ and $\left[G_{dj}^{(i,j)} \right]$ are the KICs for a given primitive pair (i,j), $\overline{\theta}$ is the joint position for the manipulator associated with primitive *i* and $\overline{\phi}$ is the joint position for the manipulator associated with primitive *j*.

If we then define the witness points $\overline{W}_i^{(i,j)}$ and $\overline{W}_j^{(i,j)}$ to be the endpoints of the line segment representing the smallest distance between two primitives, then $\left[G_{di}^{(i,j)} \right]$ and $\left[G_{dj}^{(i,j)} \right]$ can be defined as the product of the translational set of KICs relative to these witness points on each primitive and a unit vector, $\hat{d}_{i,j}$, that points from $\overline{W}_j^{(i,j)}$ to $\overline{W}_i^{(i,j)}$. This means that

$$\left[G_{di}^{(i,j)} \right] = \left[G_{p(W_i)} \right] \bullet \hat{d}_{i,j} \tag{4}$$

and

$$\left[G_{dj}^{(i,j)} \right] = -\left[G_{p(W_j)} \right] \bullet \hat{d}_{i,j} . \tag{5}$$

The matrix $\left[G_{p(W_i)} \right]$ is the set of translational KICs that relate the system inputs to the witness point on the i^{th} primitive, and $\left[G_{p(W_j)} \right]$ is the set of translational KICs that relate system inputs to the witness point on j^{th} primitive.

Similarly the second order time derivative of distance between primitives *i* and *j* can be written using first and second order KICs as

$$\ddot{d}_{(i,j)} = \left[G_{di}^{(i,j)} \right] \dddot{\theta} + \left[G_{dj}^{(i,j)} \right] \dddot{\phi} + \dot{\theta} \left[H_{di}^{(i,j)} \right] \ddot{\theta} + \dot{\phi} \left[H_{dj}^{(i,j)} \right] \ddot{\phi} + \dot{\theta} \left[H_{d(i,j)}^{(i,j)} \right] \dot{\phi} \quad (6)$$

The derivations for the second order KICs are presented in [23] and an efficient method of determining KIC values in general is presented in [22].

III. Estimated Time-to-Collision Formulation

It is now possible to formulate first and second order instantaneous estimates of the time-to-collision using the kinematic framework outlined in the previous section. It can also be inferred from the complexity of (6) that estimates based on even higher order approximations of the system will be computationally infeasible.

For a first-order approximation assuming an initial distance d_0, the distance as a function of time is

$$d(t) = vt + d_0 \quad (7)$$

Substituting in the current values for $d_{(i,j)}$ and $\dot{d}_{(i,j)}$, a first order instantaneous estimate for time-to-collision between two primitives can be written as

$$t_{(i,j)}^{est} = -\frac{d_{(i,j)}}{\dot{d}_{(i,j)}}. \quad (8)$$

Substituting the KIC relationships between the inputs and the distance primitive pair *(i, j)* outlined in the previous section, we see that

$$t_{(i,j)}^{est} = -\frac{d_{(i,j)}}{\left[G_{di}^{(i,j)} \right] \dot{\theta} + \left[G_{dj}^{(i,j)} \right] \dot{\phi}} \quad (9)$$

This metric can be used as direct substitute for $d_{(i,j)}$ in distance-based obstacle avoidance techniques. Like distance and other metrics proposed in the literature, this metric will approach zero due to an impending collision. However, the inclusion of the closing velocity in the calculation of the metric gives a more accurate representation of the current obstacle avoidance state for the system as it includes information both about the distance between manipulators as well as an approximation of how quickly the distance is closing, allowing an algorithm or human operator to distinguish between critical and non-critical distance pairs.

Similarly we can formulate a 2nd order estimate of the time-to-collision. Given an initial velocity v_0 and constant acceleration a, the distance as a function of time is

$$d(t) = \frac{1}{2} a t^2 + v_0 t + d_0 \quad (10)$$

With the knowledge of current values for $d_{(i,j)}$, $\dot{d}_{(i,j)}$ and $\ddot{d}_{(i,j)}$, a second order instantaneous estimate for time to collision between two primitives can be written as

$$t_{(i,j)}^{est} = \frac{-\dot{d} \pm \sqrt{\dot{d}^2 - 2\ddot{d}d}}{\ddot{d}} \quad (11)$$

which is completed by substituting in equations (3) and (6). It is clear that (11) is computationally expensive and yields two solutions which will require further evaluation. For example, complex conjugate solutions imply that, although the manipulators are currently approaching one another, they are accelerating at a sufficient rate away from one another to avoid collision. A potentially more relevant concern will be the numerical stability of the $\left[H_{di}^{(i,j)} \right]$ term containing primitives associated with a tele-operated manipulator, since the start/stop nature of tele-operated surgical motions may lead to large and varied changes in the velocity of a primitive on one manipulator relative to a primitive on another manipulator.

IV. Input Joint Velocity Scaling

Velocity scaling only occurs in manipulators with the lower priority in a given scenario (i.e. the scrub nurse robot). Thus we can only modify the impact its velocity has in order to maximize the time-to-collision when necessary. Thus, if one manipulator is stationary, (9) reduces to

$$t_{(i,j)}^{est} = -\frac{d_{(i,j)}}{\left[G_{di}^{(i,j)} \right] \dot{\theta}} \quad (12)$$

and (11) reduces to

$$t_{(i,j)}^{est} = \frac{-\left(G_{di}^{(i,j)} \dot{\theta} \right) \pm \sqrt{\left(G_{di}^{(i,j)} \dot{\theta} \right)^2 - 2d_{(i,j)} \left(G_{di}^{(i,j)} \ddot{\theta} + \dot{\theta}^T H_{di}^{(i,j)} \dot{\theta} \right)}}{\left(G_{di}^{(i,j)} \ddot{\theta} + \dot{\theta}^T H_{di}^{(i,j)} \dot{\theta} \right)}. \quad (13)$$

Let $\overline{T}_{(i,j)}^{est}$ be the set of all estimated time-to-collisions $t_{(i,j)}^{est}$ for all primitive pairs between manipulators, and $t_{\min}$ be the specified minimum allowable time-to-collision. If we then define $t_{(I,J)}^{est}$ as the smallest estimated time-to-collision in the set $\overline{T}_{(i,j)}^{est}$ then

$$t_{(I,J)}^{est} = -\frac{d_{(I,J)}}{\left[G_{dI}^{(I,J)} \right] \dot{\theta}}. \quad (14)$$

We can than calculate the ratio between $t_{\min}$ and $t_{(i,j)}^{est}$ as

$$\frac{t_{(I,J)}^{est}}{t_{\min}} = \frac{d_{(I,J)}}{G_{dI}^{(I,J)} \bullet \dot{\theta}} \frac{G_{dI}^{(I,J)} \bullet \dot{\theta}'}{d_{(I,J)}} = \frac{G_{dI}^{(I,J)} \bullet \dot{\theta}'}{G_{dI}^{(I,J)} \bullet \dot{\theta}} \quad (15)$$

where $\dot{\bar{\theta}}$ is the initial joint velocity of the system and $\dot{\bar{\theta}}'$ is the required velocity to maintain the minimum time-to-collision $t_{\min}$. Using this relationship $\dot{\bar{\theta}}'$ can be calculated from $\dot{\bar{\theta}}$ as

$$\dot{\bar{\theta}}' = \frac{t^{est}_{(I,J)}}{t_{\min}} \dot{\bar{\theta}} \tag{16}$$

This result allows a joint velocity $\dot{\bar{\theta}}$ to be scaled to an alternate joint velocity $\dot{\bar{\theta}}'$, using the smallest estimated time-to-collision metric of (8), which will maintain the user specified minimum time to collision $t_{\min}$.

Because the instantaneous mapping of joint velocities to velocities in task space is linear, a similar relationship can be written for end-effector velocity scaling.

V. Null Space Optimization

. There are two key advantages to using a criterion derived from $\bar{T}^{est}_{(i,j)}$ when exploiting redundancies in the manipulator system.

- They account for implicit directionality when attempting to find a direction around an obstacle. In other words, by including the higher order properties of $d_{(i,j)}$, we can better choose joint configurations taking into account whether our motion is towards, or away from, the obstacle.
- Although computationally expensive, $\bar{T}^{est}_{(i,j)}$ is already calculated in order to perform velocity scaling, even if the metric's effectiveness is similar to others in the literature.

Many methods exist for searching a redundant manipulator's null space in order to optimize for obstacle avoidance and other metrics [2][3][19]. For example, [3] demonstrates a simple direct search method that maximizes the distance between manipulator and environment primitives in tandem with other performance objectives, such as avoiding joint limits. One described metric takes the form of an aggregate of inverse distances, and can be referred to as the Average Reciprocal Minimum Distance, or ARMD, which is defined by

$$ARMD = \frac{1}{MN} \sum_{i=1}^{M} \sum_{j=1}^{N} \frac{1}{d_{(i,j)}} \tag{17}$$

where *M* is the total number of manipulator primitives and *N* is the total number of environment primitives.

Because the estimated time-to-collision metrics in (12) and (13) exhibit the same properties as the distance metric, it can be substituted into (17) resulting in the Average Reciprocal Estimated Time-to-Collision criterion, or *ARTC*.

$$ARTC = \frac{1}{MN} \sum_{i=1}^{M} \sum_{j=1}^{N} \frac{1}{t^{est}_{(i,j)}} \tag{18}$$

Because this criterion works to maximize the estimated time-to-collision, it will give more efficient results than those obtained from ARMD. In other words, movements within the null space which cause primitive pair distances to increase at a high rate of speed are given a higher priority, which is not true in criteria based only on distance. This distinction is especially important in manipulators with many extra degrees of freedom, where more complex movements are possible and more easily managed.

VI. Collision Detection

The third leg of the proposed collision avoidance strategy is a final check for collisions in the system, which can be simply stated as $d_{(i,j)} \le d_{\min}$ for all $\bar{D}_{(i,j)}$ where $\bar{D}_{(i,j)}$ is the set of all primitive-to-primitive distance calculations and $d_{\min}$ is a user specific allowable approach distance.

Due to the compact workspace and the close proximity of the manipulators, the low resolution cylisphere model must be replaced with a high resolution geometry model for collision detection. In practice, these models are derived from the CAD models of the system components and the collision detection algorithms are run in a separate computational process than the robot decision making system as an additional factor of safety. [24]

VII. Implementation and Simulation

The presented techniques for input velocity scaling, null space optimization and collision detection were simulated in a multiple manipulator workcell. The manipulators are fixed with base locations very close relative to their workspace volumes, presenting many opportunities for collision. Both manipulators are Mitsubishi PA10-7C seven degree-of-freedom serial robots as shown in Figure 2. The left manipulator, representing an autonomous support (i.e. nurse) manipulator, was directed along the path shown in the Figure 2. The other, referred to as the priority (i.e. surgical) manipulator is thus approached by the support manipulator representation of a task where an item or tool is exchanged.

During the simulation, the end-effector velocity of the support manipulator was scaled to maintain a minimum estimated time-to-collision between the manipulators. At the same time, both manipulator configurations were optimized within their null space in order to avoid collisions. The performance criterion used for the optimization was the Average Reciprocal Estimated Time to Collision metric presented in the previous section. The simulation was completed using UTA's Operational Software for Advanced Robotics (OSCAR) [25][26] and Roboworks [27] for

visualization. The simulation path was selected to demonstrate all three techniques during a single task.

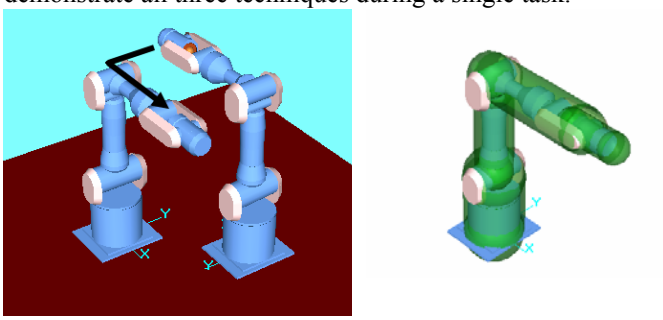

Fig. 2. Initial configuration and cylisphere model for each the manipulator workspace. For this simulation, the left PA-10 is considered the surgical (priority) manipulator. The arrow represents the approximate path the nurse manipulator will follow to as it approaches the priority manipulator's EEF.

Because the current movement of the priority manipulator is unknown to the support manipulator, the formulation of estimated time-to-collision that assumes static environment obstacles was used for optimizing the supporting robot's configuration. Once the velocity state of the support manipulator is calculated, the combined kinematic information was then used to determine the movement of the priority manipulator.

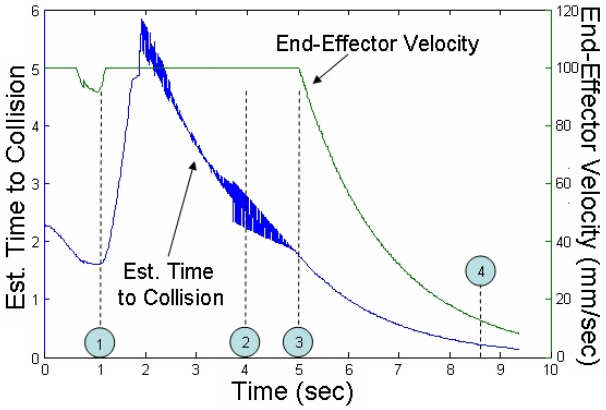

Fig. 3. Impact of $t^{est}_{(I,J)}$ on the magnitude of the support manipulator's EEF velocity during the prescribed path. Configurations at the time stamps 1-4 are illustrated in Figure 5.

When the prescribed path brings the nurse manipulator's EEF near the elbow of the priority manipulator, the effects of both velocity scaling and obstacle avoidance via self motions in the surgical manipulator are observed, automatically preventing a collision while maintaining the end-effector position and orientation of the priority manipulator. The velocity scaling and relative values of the null space metric are shown in Figures 3 and 4. Note the oscillations in $t^{est}_{(I,J)}$ were due to switching between witness points in the minimum distance calculations. Practical experience demonstrated this was not an issue when the $t^{est}_{(I,J)}$ was small enough to warrant EEF velocity scaling.

A second opportunity for collision occurs as the end-effectors approach each other at the end of the prescribed path. Since the complete position and orientation information for both end-effectors is specified, null space optimization can not prevent the collision (in fact, if the task is to exchange an item or tool, a 'collision' is the desired outcome of the move). Instead the end-effector velocity is scaled as the EEFs approach one another after the user defined minimum estimated time-to-collision boundary is violated. At this point the velocity of the support manipulator was slowed, causing the estimated time to collision to stay constant despite the decreasing minimum distance between the manipulators. Because the minimum distance between the manipulators is calculated within the estimated time to collision metric, it can easily be monitored preventing an actual collision.

In reality, this collision pair may be exempted from the final check if the task dictates an interaction. Additionally, because the velocity of the support manipulator will be continuously decreasing due to velocity scaling, the halt command will be the final step of the velocity profile that approaches zero, preventing a sudden jerk due to the emergency stop.

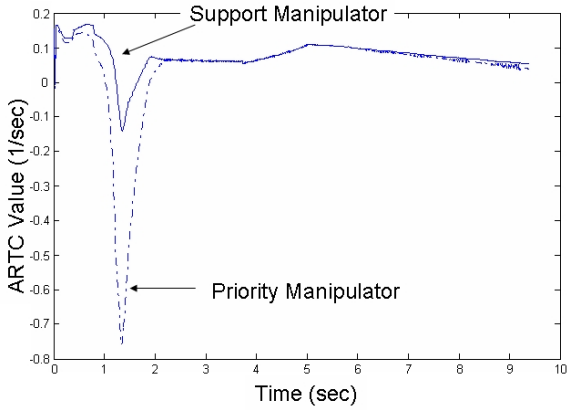

Fig. 4. The value of the null-space optimization metric ARTC for both manipulators during the prescribed path.

Another positive aspect of this velocity scaling technique is that it accounts for the directional aspect of the obstacle avoidance problem. If the support manipulator starts a short distance away from the surgical manipulator and its end-effector is commanded to move in a way that decreases this distance, the estimated time-to-collision will be small causing the scaling algorithm to slow the movement and maintain safety within the workcell. Reciprocally, if a command increases the distance, the constraint imposed by the user specified minimum estimated time-to-collision will not be violated and the manipulator will be allowed to move away at full speed. This intuitive behavior would not occur with an obstacle avoidance metric based solely on scalar distance between the manipulators which did not include its higher order properties.

VIII. Conclusion

This paper reviews several techniques that allow multiple robots – tele-robotic and autonomous – to avoid collisions and impasse scenarios when working in a compact workspace. Of particular interest is a workspace that contains one or more arms tele-operated by a surgeon that are supported by one or more supporting manipulators that transport tools and supplies to and from the surgical site.

These techniques were then presented in a simple workcell that contained two 7DOF manipulators with their bases fixed in close proximity. A simple task was then selected that demonstrated all three proposed techniques (velocity scaling, null-space optimization, and collision detection) all using the single metric that estimates the time-to-collision between manipulators in the workcell.

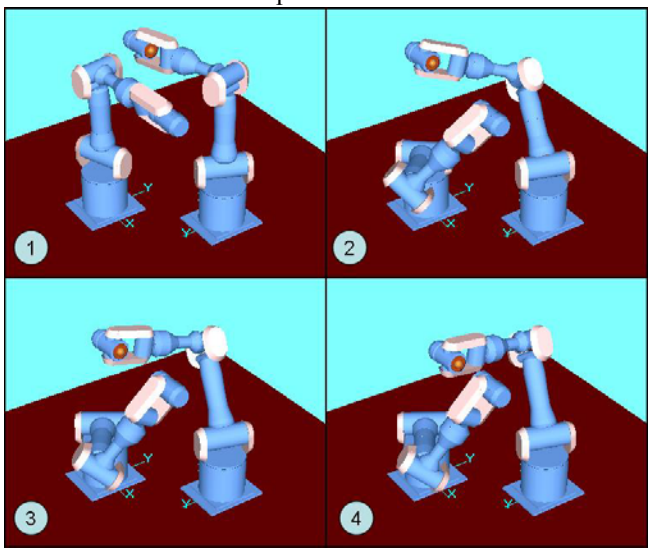

Fig. 5. Representative workcell configurations at four key instances noted in Figure 3.

The path and configurations shown in this simulation provide a clear visualization as well as performance data which illustrate salient aspects of the algorithms. These methods will further advance our goal of an operating room where the patient is the only individual in the room.

Acknowledgment

The authors would like to acknowledge all those who have contributed to the development of OSCAR. In particular we would like to thank Troy Harden and Ethan Swint for their foundational work in obstacle avoidance at the University of Texas at Austin.

References

[1] O. Khatib, "Real-Time obstacle avoidance for manipulators and mobile robots," *Int. J. of Robotics Research*, 1986, 5(1):90-98.

[2] A. Maciejewski, and C. Klein, "Obstacle avoidance for kinematically redundant manipulators in dynamically varying environments," *Int. J. of Robotics Research*, 1985, 4(3):109-117.

[3] T. Harden, C. Kapoor, and D. Tesar. "Experimental evaluation of a criteria-based obstacle avoidance scheme," *ASME Design and Eng. Tech. Conf.*, DETC99/DAC-8657, Sept. 1999.

[4] F. Schwarzer, M. Saha, J. Latombe, "Adaptive dynamic collision checking for single and multiple articulated robots in complex environments," *IEEE Tran. on Robotics*, June 2005, pp 338-353.

[5] B. Mitrich, J. Canny, "Impulsed-based simulation of rigid bodies," Int. Symposium on Interactive 3D Graphics, Monterey, CA. 1995.

[6] X. Zhang, S. Redom, M. Lee, Y. Kim, "Continuous collision detection for articulated models using Taylor models and temporal cutting," Int. Conf. on Computer Graphics and Interactive Techniques (SIGGRAPH), San Diego, CA, 2007.

[7] E. Bernabeu, "Fast generator of multiple collision-free trajectories in dynamic environment," *IEEE Int. Conf. on Robotics and Automation*, May 2006, pp. 2360-2365.

[8] M. Ali, N. Babu, K. Varghese, "Offline path planning of cooperative manipulators using co-evolutionary genetic algorithm," *Int. Sym. on Automation and Robotics in Construction,* Sept. 2002, pp, 415-424.

[9] O. Brock, O. Khatib, S. Viji, "Task-consistent obstacle avoidance and motion behavior for mobile manipulation," *IEEE Int. Conf. on Robotics and Automation*, 2002, pp. 388-393.

[10] L. Zlajpah, and B. Nemen, "Kinematic control algorithms for on-line obstacle avoidance for redundant manipulators," *IEEE Int. Conf. on Intelligent Robots and Systems*, Sept. 2002, pp. 1898-1903.

[11] D. Albocher, U. Sarel, Y. Choi, G. Elber, W. Wang, "Efficient continuous detection for bounding box under rational motion," *IEEE Int. Conf. on Robotics and Automation*, May 2006, pp. 3017-3022.

[12] M. Lim, J. Canny, "A fast algorithm for incremental distance calculation," *IEEE Int. Conf. on Robotics and Automation*, 1991, pp 1009-1014.

[13] M. Sugiura, M. Gienger, H. Janssen, and G. Christian, "Real-time self collision avoidance for humanoids by means of nullspace criteria," *Int. Con. on Humanoid Robots*, 2006, pp. 575-580.

[14] S. Kwon, W. Chung, M. Kim, "Self-collision avoidance for n-link redundant manipulators," *IEEE International Conference on Systems, Man, and Cybernetics,* 1991, pp. 937-942.

[15] T. Fraichard, "A short paper about motion safety," *IEEE Int. Conf. on Robotics and Automation*, 2007, pp. 1140-1145

[16] S. Morikawa, T. Senoo, A. Namiki, and M. Ishikawa, "Realtime collision avoidance using a robot manipulator with light-weight small high-speed vision cameras," *IEEE Intl Conf. on Robotics and Automation*, 2007, pp. 794-799.

[17] W. Yu, R. Alqasemi, R. Dubey, and N. Pernalete, "Telemanipulation assistance based on motion intention recognition," *IEEE Int. Conf. on Robotics and Automation,* 2005, pp. 1121-1126.

[18] D. Aarno, S. Ekvall, and D. Kragic, "Adaptive virtual fixtures for machined-assisted teleoperation tasks," *IEEE Int. Conf. on Robotics and Automation,* 2005, pp. 1139-1144.

[19] O. Brock, and O. Khatib, "Real-time obstacle avoidance and motion coordination in a multi-robot workcell," *IEEE Int. Conf. on Robotics and Automation,* 1999, pp. 274-279.

[20] R. Dubey, S. Everett, N. Pernalete, and K. Manocha, "Teleoperation assistance through variable velocity mapping," *IEEE Trans. on Robotics and Automation*, October 2001, pp. 761-766.

[21] S. Choi, and B. Kim, "Obstacle avoidance for redundant manipulators using collidability measure", *Robotica*, 2000, 18:143-151.

[22] M. Thomas, and D. Tesar, "Dynamic modeling of serial manipulator arms," *J. of Dyn. Sys., Meas., and Control*, 1982, 102:218-228.

[23] A. Spencer, C. Kapoor, and D. Tesar, "Obstacle Avoidance for multiple robot systems," Masters thesis, Dept. Mech. Eng., Univ. of Texas at Austin, Austin, TX, www.robotics.utexas.edu, 2007.

[24] J. Knoll, C. Kapoor, and D. Tesar, "Geometric workcell modeling for robot control and coordination," Masters thesis, Dept. Mech. Eng., Univ. of Texas at Austin, Austin, TX, 2007.

[25] C. Kapoor, M. Cetin, M. Pryor, C. Cocca, T. Harden, and D. Tesar, "A software architecture for multi-criteria decision making for advanced robotics," *IEEE Int. Sym. on Comp. Int. in Robotics and Automation, Int. Sys., and Semiotics,* September, 1998, pp. 525-530.

[26] C. Kapoor, and D. Tesar, "Integrated teleoperation and automation for nuclear facility cleanup," *Industrial Robot: an International Journal*, 2006, 33(6):469-484.

[27] C. Kapoor, Roboworks. www.newtonium.com.